Results from PVLAS

Guido Zavattini
Università di Ferrara and INFN-Ferrara

On behalf of the PVLAS collaboration

Summary

- Introduction and aim of the PVLAS experiment
  - Vacuum magnetic birefringence
  - Axion search
- Experimental method
  - Heterodyne technique
  - Fabry-Perot interferometer
- The PVLAS experiment in Ferrara
- Results
- Future

Aim of the PVLAS experiment

Light propagation in an external field

- Experimental study of the propagation of light in vacuum in an external field

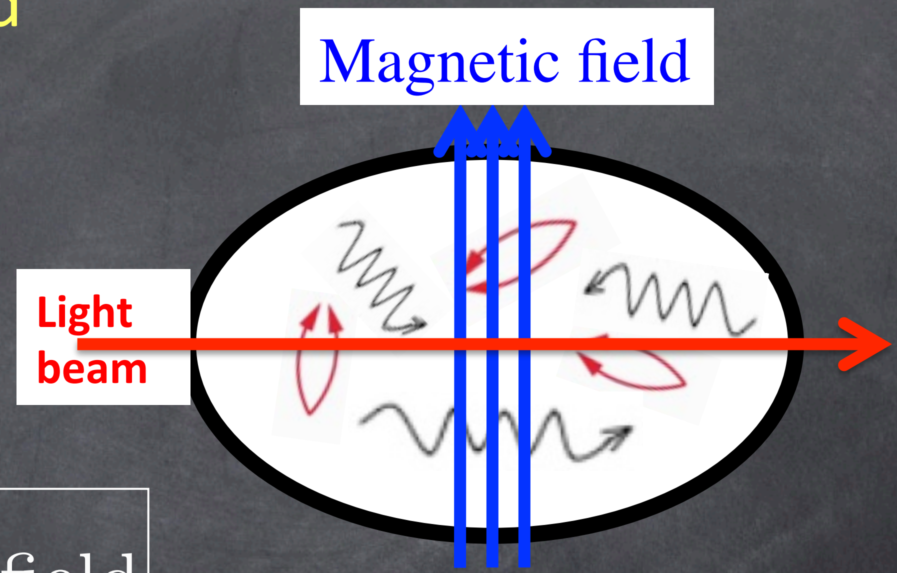

We are aiming at measuring **variations of the index of refraction** in vacuum due to the external **magnetc** field

$$\boxed{n_{\mathrm{vac}} = 1 + (n_{\mathrm{B}} - i\kappa_{\mathrm{B}})_{\mathrm{field}}}$$

The full program of the PVLAS experiment is to detect and measure

- **LINEAR BIREFRINGENCE**
- **LINEAR DICHROISM**

acquired by vacuum induced by an external magnetic field **B**

Linear birefringence

- A birefringent medium has $n_{||} \neq n_{\perp}$
- A linearly polarized light beam propagating through a birefringent medium will acquire an ellipticity ψ

If the light polarization forms an angle ϑ with respect to the magnetic field **B** the electric field of the laser beam before and after can be expressed as

$$\vec{E}_\gamma = E_\gamma \begin{pmatrix} 1 \\ 0 \end{pmatrix}$$

After a phase delay ϕ of the component parallel to **B** with respect to the component perpendicular to **B**

$$\phi = \frac{2\pi}{\lambda}(n_\parallel - n_\perp)L$$

$$\vec{E}_\gamma \simeq E_\gamma \begin{pmatrix} 1 \\ i\frac{\phi}{2}\sin 2\vartheta \end{pmatrix}$$

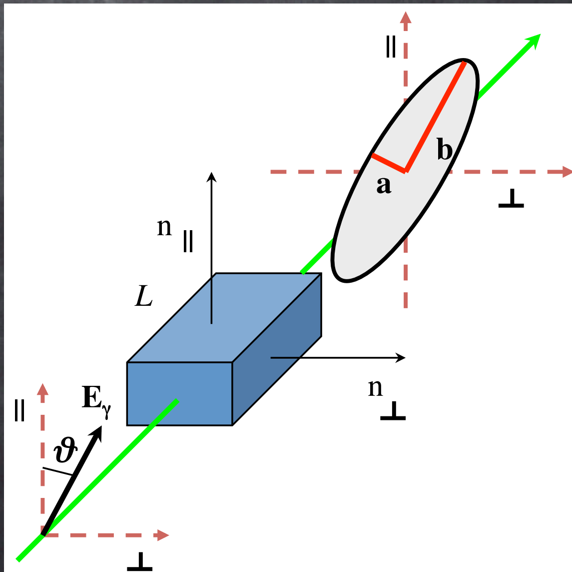

Ellipticity

$$\boxed{\psi = \frac{a}{b} \approx \frac{\pi \Delta n L}{\lambda} \sin 2\vartheta}$$

Linear dichroism

- A dichroic medium has different extinction coefficients: $\kappa_{||} \neq \kappa_{\perp}$
- A linearly polarized light beam propagating through a dichroic medium will acquire an apparent **rotation** ε

If the ligh polarization forms an angle ϑ with respect to the magnetic field **B** the electric field of the laser beam before and after can be expressed as

$$\vec{E}_\gamma = E_\gamma \begin{pmatrix} 1 \\ 0 \end{pmatrix}$$

After a reduction of the field component parallel to **B** with respect to the component perpendicular to **B** by

$$q - 1 = \frac{2\pi}{\lambda}(\kappa_{\|} - \kappa_{\perp})L$$

$$\vec{E}_\gamma \simeq E_\gamma \begin{pmatrix} 1 \\ \frac{q-1}{2} \sin 2\vartheta \end{pmatrix}$$

Apparent rotation

$$\boxed{\epsilon \approx \left(\frac{q-1}{2}\right) \sin 2\vartheta = \frac{\pi \Delta\kappa L}{\lambda} \sin 2\vartheta}$$

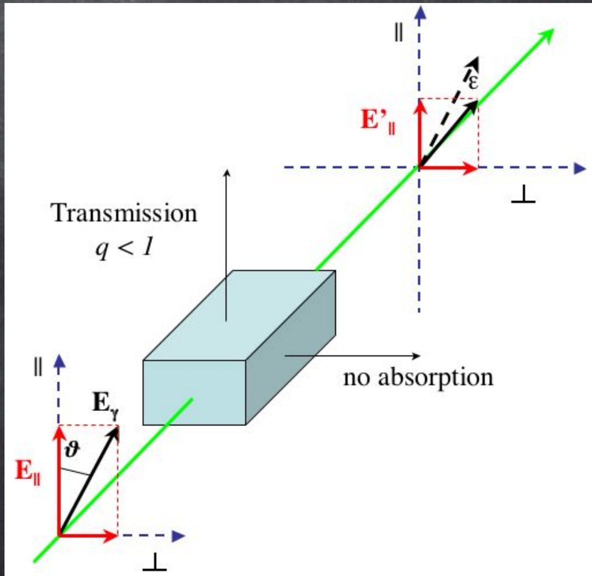

Heisenberg, Euler, Kochel and Weisskopf ('36)

They studied the electromagnetic field in the presence of the virtual electron-positron sea discussed a few years before by Dirac. The result of their work is an effective Lagrangian density describing the electromagnetic interactions. At lowest order (Euler – Kochel):

$$\boxed{\mathcal{L}_{\mathrm{EH}} = \frac{1}{2\mu_0}\left(\frac{\vec{E}^2}{c^2} - \vec{B}^2\right) + \frac{A_e}{\mu_0}\left[\left(\frac{\vec{E}^2}{c^2} - \vec{B}^2\right)^2 + 7\left(\frac{\vec{E}}{c}\cdot\vec{B}\right)^2\right] + \dots}$$

$$\boxed{A_e = \frac{2}{45\mu_0}\frac{\alpha^2 \lambda\!\!\!^{-}{}_e^3}{m_e c^2} = 1.32 \times 10^{-24}\ \mathrm{T}^{-2}.}$$

H Euler and B Kochel, *Naturwissenschaften* **23**, 246 (1935)
W Heisenberg and H Euler, *Z. Phys.* **98**, 714 (1936)
H Euler, *Ann. Phys.* **26**, 398 (1936)
V Weisskopf, *Mat.-Fis. Med. Dan. Vidensk. Selsk.* **14**. 6 (1936)

Which is valid for:

1) slowly varying fields
2) fields smaller than their critical value ($B \ll 4.4\cdot10^9$ T; $E \ll 1.3\cdot10^{18}$ V/m)

In the presence of an external field vacuum is polarized. It became evident that photon – photon interactions could occur in vacuum.

This lagrangian was **validated in the framework of QED by Schwinger** (1951), and the processes described by it can be represented using Feynman diagrams.

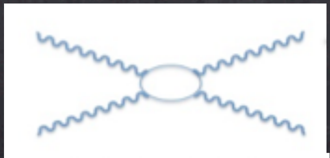

Index of refraction - birefringence

$$n_{\mathrm{B},\parallel} \text{ and } n_{\mathrm{B},\perp} \neq 0$$
$$n_{\mathrm{B},\parallel} - n_{\mathrm{B},\perp} \neq 0$$

- $v \neq c$
- anisotropy

$$\boxed{n_\parallel - n_\perp = 3A_e B^2}$$

Numerically

$$n_\parallel - n_\perp = 2.5 \times 10^{-23} \text{ @ } B = 2.5\,\mathrm{T}$$

QED also predicts dichroism due to photon splitting in an external magnetic field *but* it is unmeasureably small.

Axion like particles

Axion-like particles

One can add extra terms [*] to the E-H effective lagrangian to include contributions from hypothetical **neutral light particles interacting weakly with two photons** (Heaviside – Lorentz units)

$$L_\phi = g_\mathrm{a}\phi\left(\vec{E}_\gamma \cdot \vec{B}_\mathrm{ext}\right)$$

pseudoscalar case: Interaction if polarization is parallel to B_{ext}

g_a, g_s are the coupling constants

$$L_\sigma = g_\mathrm{s}\sigma\left(\vec{B}_\gamma \cdot \vec{B}_\mathrm{ext}\right)$$

scalar case: Interaction if polarization is perpendicular to B_{ext}

Effects on photon propagation

The photon will oscillate with the axion

Absorption

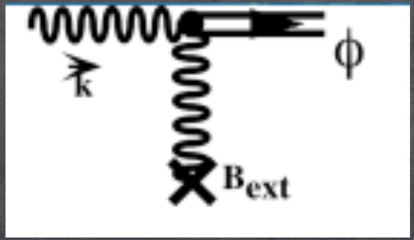

DICHROISM

Dispersion

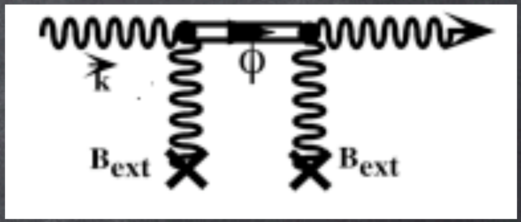

BIREFRINGENCE

[L.Maiani, R. Petronzio, E. Zavattini, Phys. Lett B, Vol. 173, no.3 1986]
[E. Massò and R. Toldrà, Phys. Rev. D, Vol. 52, no. 4, 1995]

Axion-like particles (pseudoscalar)

- Dichroism induces an apparent rotation ε

$$\boxed{\epsilon = -\sin 2\vartheta \left(\frac{g_{\mathrm{a,s}} L}{4}\right)^2 B_{\mathrm{ext}}^2 N \left(\frac{\sin x}{x}\right)^2}$$

N = number of passes through the magnetic field

- Birefringence induces an ellipticity ψ

$$\boxed{\psi = \sin 2\vartheta \frac{g_{\mathrm{a,s}}^2 k L}{4 m_{\mathrm{a,s}}^2} B_{\mathrm{ext}}^2 N \left(1 - \frac{\sin 2x}{2x}\right)}$$

Units

$$1\ \mathrm{T} = \sqrt{\frac{\hbar^3 c^3}{e^4 \mu_0}} = 195\ \mathrm{eV}^2$$

$$1\ \mathrm{m} = \frac{e}{\hbar c} = 5.06 \cdot 10^6\ \mathrm{eV}^{-1}$$

Where $x = \frac{L}{2}\left[\frac{m_{\mathrm{a,s}}^2}{2k}\right]$ and *k* is the wave number

- Both ε and ψ are proportional to N
- Both ε and ψ are proportional to B^2
- ε depends only on $g_{a,s}$ for small x
- **the ratio ψ / ε depends only on $m^2_{a,s}$**

Both $g_{a,s}$ and $m_{a,s}$ can be disentangled

Summing up ...

Dichroism Δκ

- Real particle production
- (Photon splitting)

Birefringence Δn

- QED dispersion
- Virtual particle production

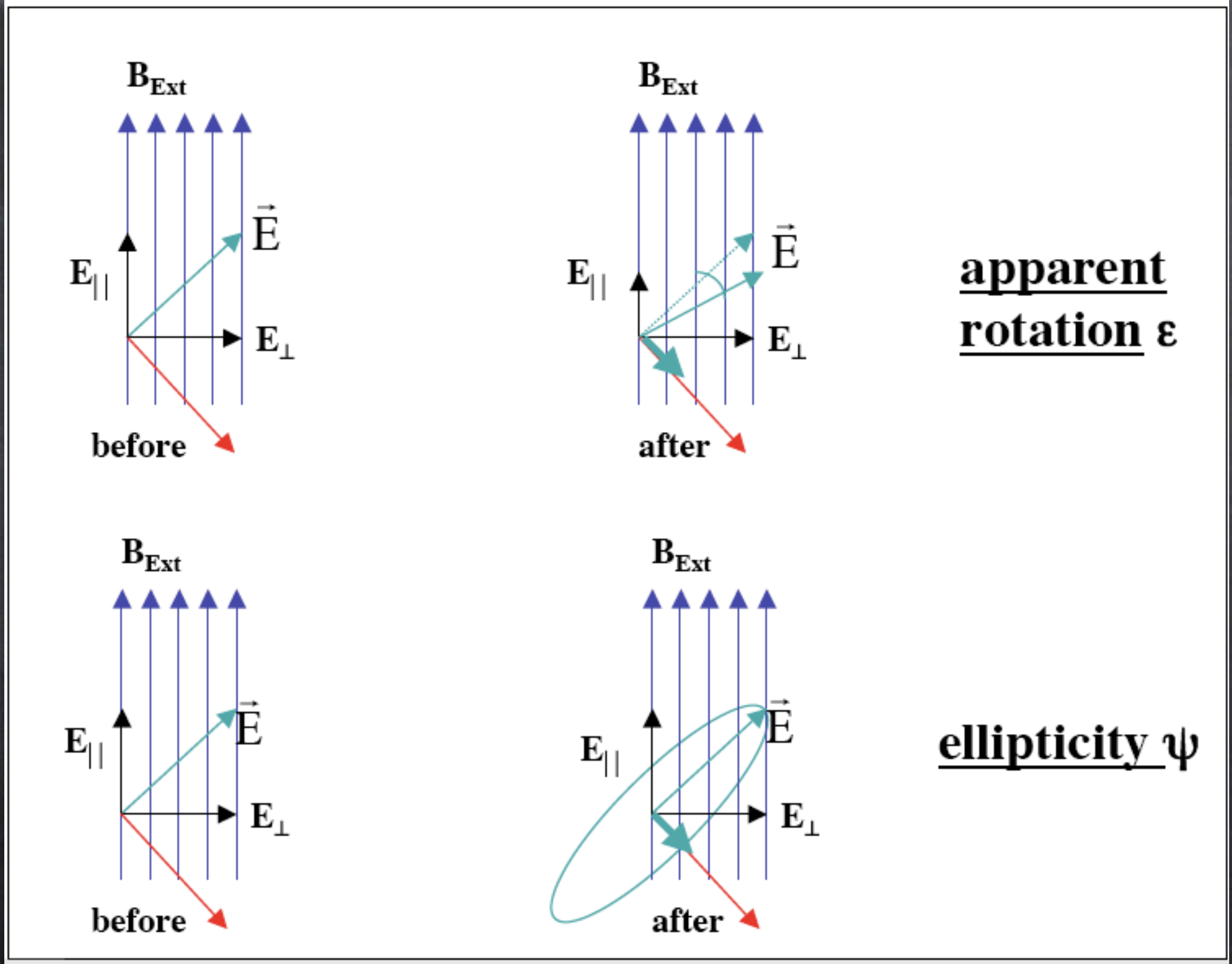

Both Δn and Δκ are defined with sign

Heterodyne detection

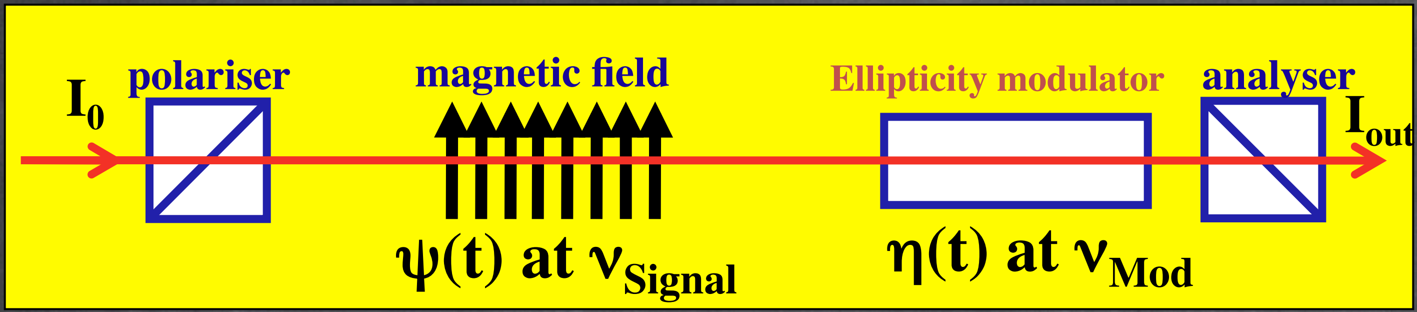

- The Intensity measured at the output is $$I = \vec{E}^T \cdot \vec{E}^*$$

- Small ellipticities add up. Let us therefore add a known time dependent ellipticity with a modulator placed with ϑ = 45°

$$\vec{E}_{\rm out} = E_0 \begin{pmatrix} 0 \\ i\psi \sin 2\vartheta + i\eta(t) \end{pmatrix}$$

Making ϑ time dependent by rotating the magnetic field

$$\boxed{I_{\rm out} \simeq I_0 \left[\eta(t)^2 + 2\eta(t)\psi \sin 2\vartheta(t) + ...\right]}$$

The intensity <u>is linear in ψ</u>

Fourier spectrum

In practice, nearly static ellipticities $\alpha(t)$ generate a 1/f noise centered around ν_{Mod}. Including the polarizers' extinction ratio σ^2

$$I_{Tr} = I_0\left[\sigma^2 + \left(\psi(t) + \eta(t) + \beta_s(t)\right)^2\right]$$

$$= I_0\left[\sigma^2 + \left(\eta(t)^2 + \underbrace{2\psi(t)\eta(t)}_{\text{signal}} + \underbrace{2\alpha(t)\eta(t)}_{\text{noise}} + \dots\right)\right]$$

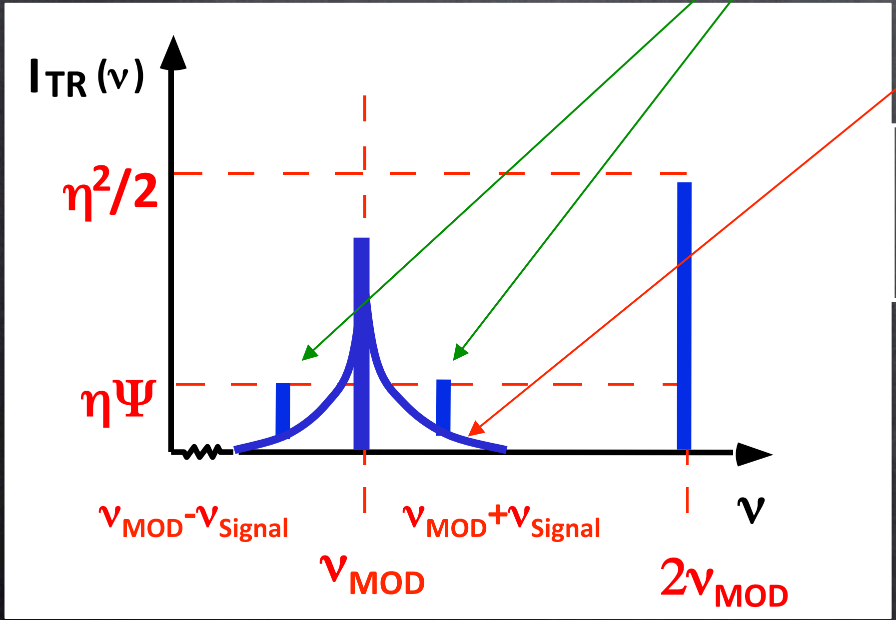

Main frequency components at $\nu_{Mod} \pm \nu_{Signal}$ and $2\nu_{Mod}$

Signal amplification

- To increase the optical path length within the magnetic field a Fabry-Perot cavity is used. The amplification factor is

$$N = \frac{2\mathcal{F}}{\pi}$$

where $\mathcal{F}$ is the finesse of the cavity.

$$\mathcal{F} = \frac{\nu_{\mathrm{fsr}}}{\Delta\nu_{\mathrm{cav}}}$$

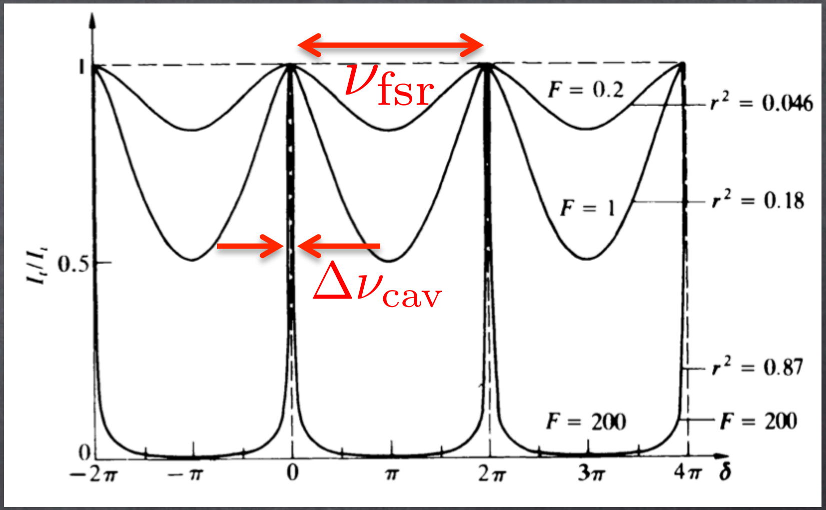

- The intensity then will be

$$\boxed{I_{\mathrm{out}} \simeq I_0 \left[\sigma^2 + \eta(t)^2 + 2\eta(t)\left(\frac{2\mathcal{F}}{\pi}\right)\psi \sin 2\vartheta(t) + 2\eta(t)\alpha(t) \ldots\right]}$$

Ellipiticity vs Rotations

- Ellipticities have an imaginary component whereas rotations are real. In the presence of an induced rotation ε and an ellipticity modulator η, the electric field after the analyzer is

$$\vec{E}_{\mathrm{out}} \simeq E_0 \begin{pmatrix} 0 \\ \epsilon + i\eta \end{pmatrix}$$

- The intensity will be

$$\boxed{I_{\mathrm{out}} = I_0 |\epsilon + i\eta|^2 = I_0(\epsilon^2 + \eta^2)}$$

In principle rotations do not beat with ellipticities

Rotation measurement

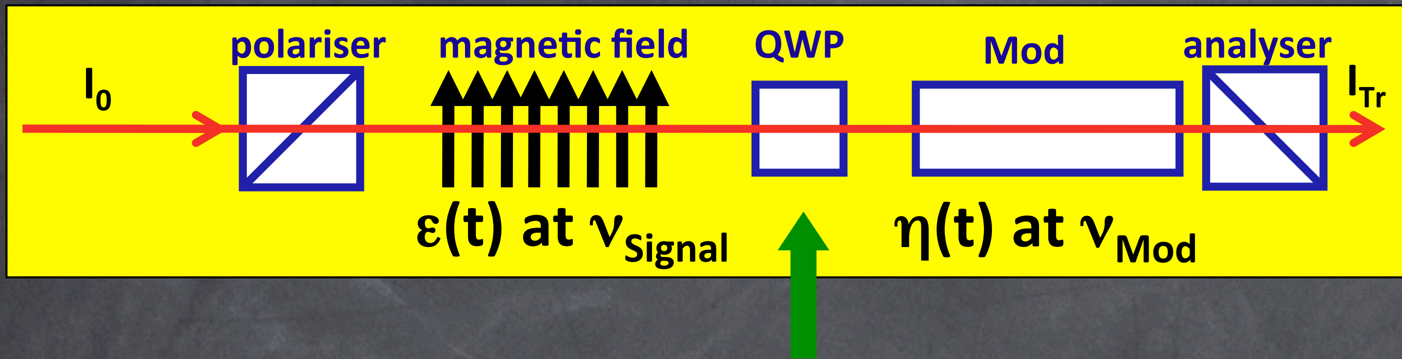

QWP can be inserted to transform a rotation ε into an ellipticity ψ with the same amplitude. It can be oriented in two positions:

QWP axis along polarization
QWP axis normal to polarization

$$\epsilon(t) \Rightarrow \begin{cases} \psi(t) & \text{for QWP } \parallel \\ -\psi(t) & \text{for QWP } \perp \end{cases}$$

$$\boxed{I_{\rm out} \simeq I_0\left[\sigma^2 + \eta(t)^2 \pm 2\eta(t)\left(\frac{2\mathcal{F}}{\pi}\right)\epsilon\sin 2\vartheta(t) + 2\eta(t)\alpha(t)...\right]}$$

Main frequency components at $\nu_{Mod} \pm \nu_{Signal}$ and $2\nu_{Mod}$

PVLAS scheme

- The Fabry-Perot cavity will increase the single pass ellipticity by a factor $N = \dfrac{2\mathcal{F}}{\pi}$
- The heterodyne detection linearizes the ellipticity ψ to be measured
- The rotating magnetic field will modulate the searched effect

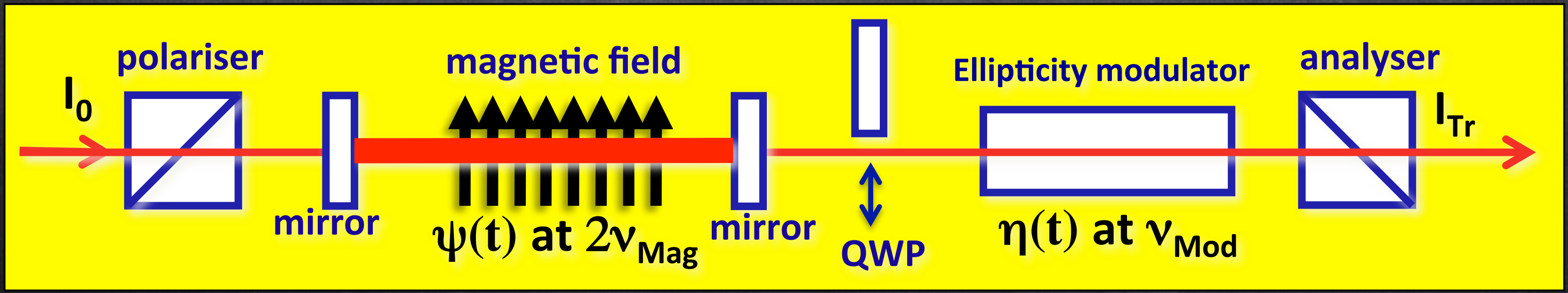

Experimental parameters

- Wavelength = 1064 nm
- $\int_0^L B_{\text{Ext}}^2 dl = 10.25$ $\mathrm{T^2m}$; B_{Ext} = 2.5 T, L = 1.6 m
- Magnet rotation frequency 3-20 Hz
- Present finesse = 710000.
- Vacuum: ≈ 10^{-8} mbar
- Expected QED ellipticity signal: $5.4\cdot10^{-11}$

The magnets

Halbach configuration

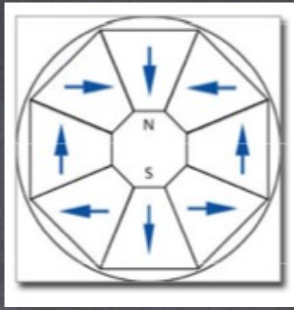

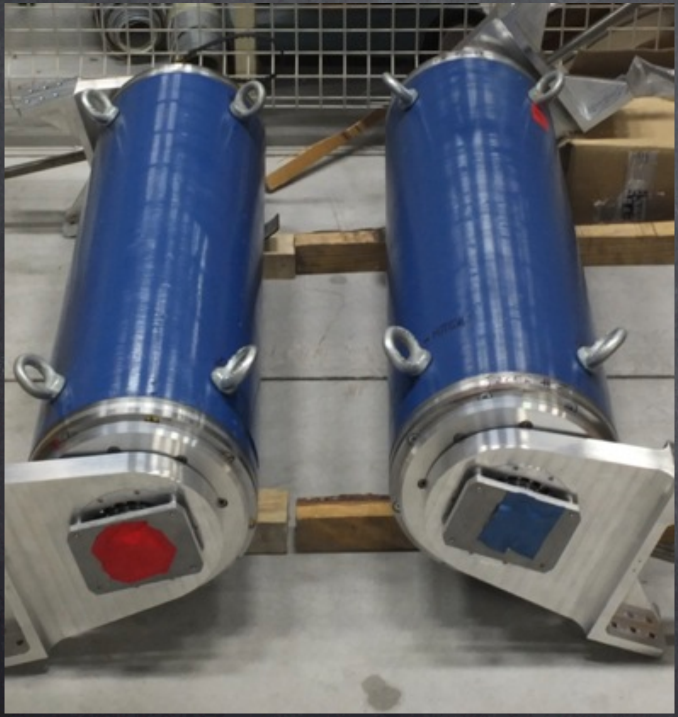

Total field integral = (10.25±0.06) T^2m

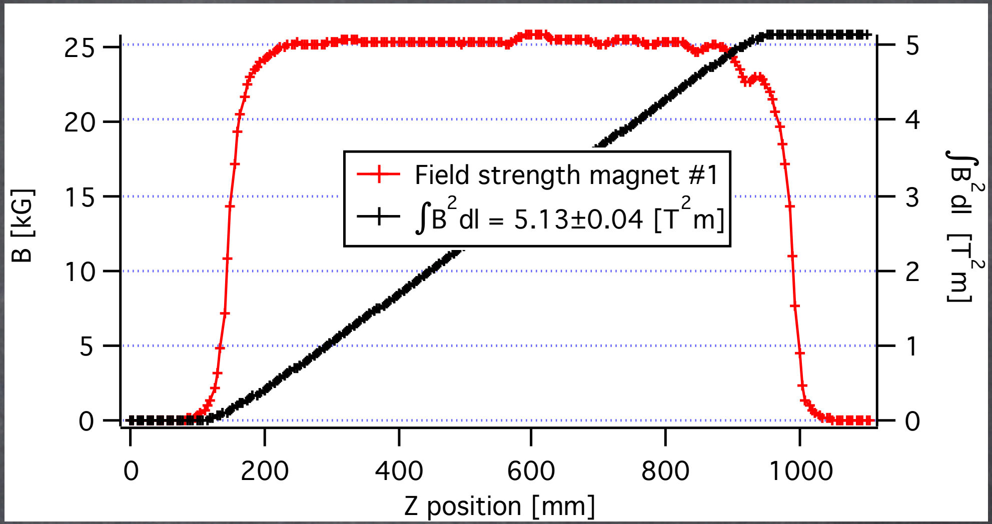

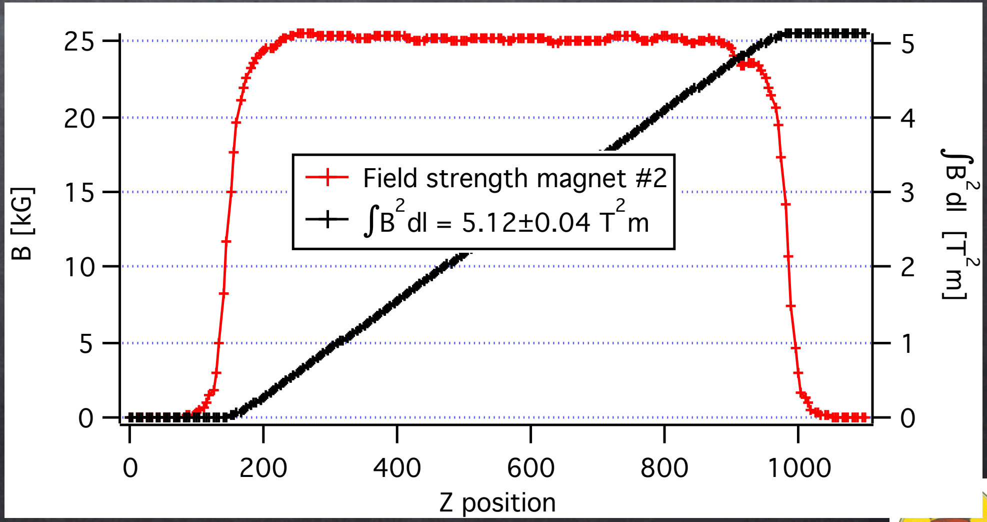

Magnets have built in **magnetic shielding**

Stray field below 1 Gauss on side

Vacuum and pumping

- All components of the vacuum system and optical mounts made with **non magnetic materials** (at best)
- Vacuum pipe through magnet made in **Pyrex** to avoid eddy currents
- Pyrex pipe externally varnished with black paint to avoid interaction of scattered light with magnets
- Baffles inside the Pyrex tubes to reduce diffused light
- Motion of optical components inside vacuum chamber by means of **piezo-motor**
- High vacuum obtained with getter - NEG pumps – **noise free, magnetic field free**

Vacuum chambers

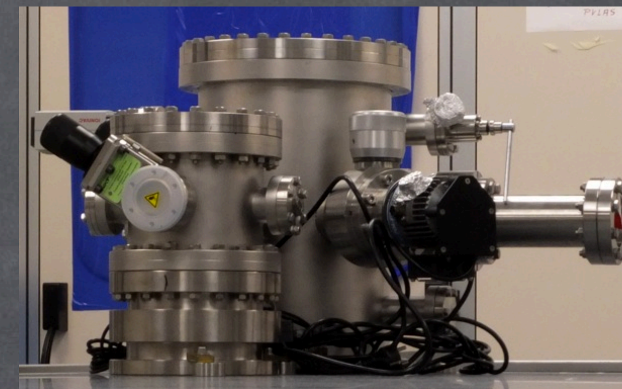

Linear translator

Getter pumps

Optics layout

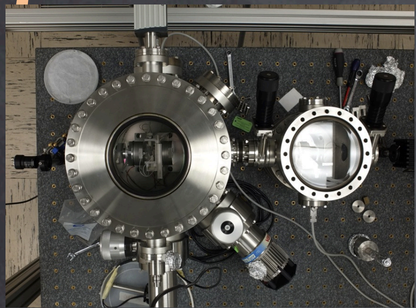

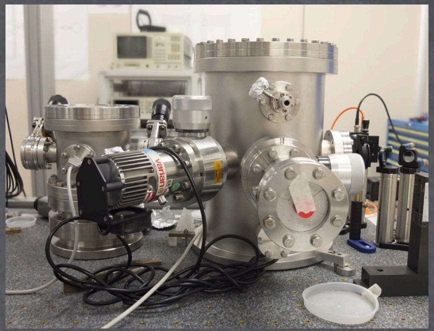

3.3 m long Fabry Perot cavity

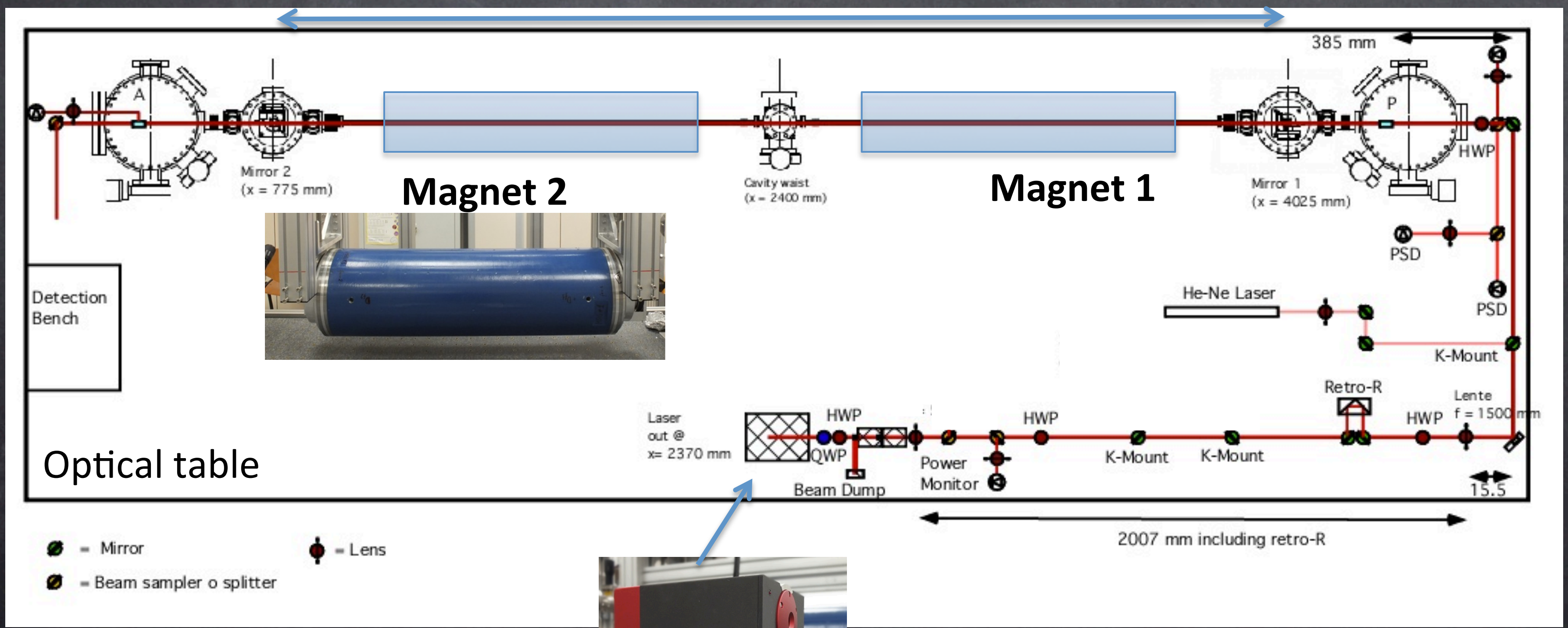

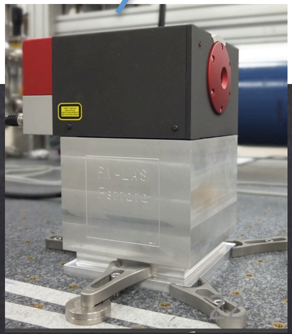

2 W NPRO Nd:Yag Laser
λ = 1064 nm

Cavity

- Fabry Perot cavity high finesse mirrors
- Spherical mirror with r = − 2 m
- Automatic locking system to allow long integration times

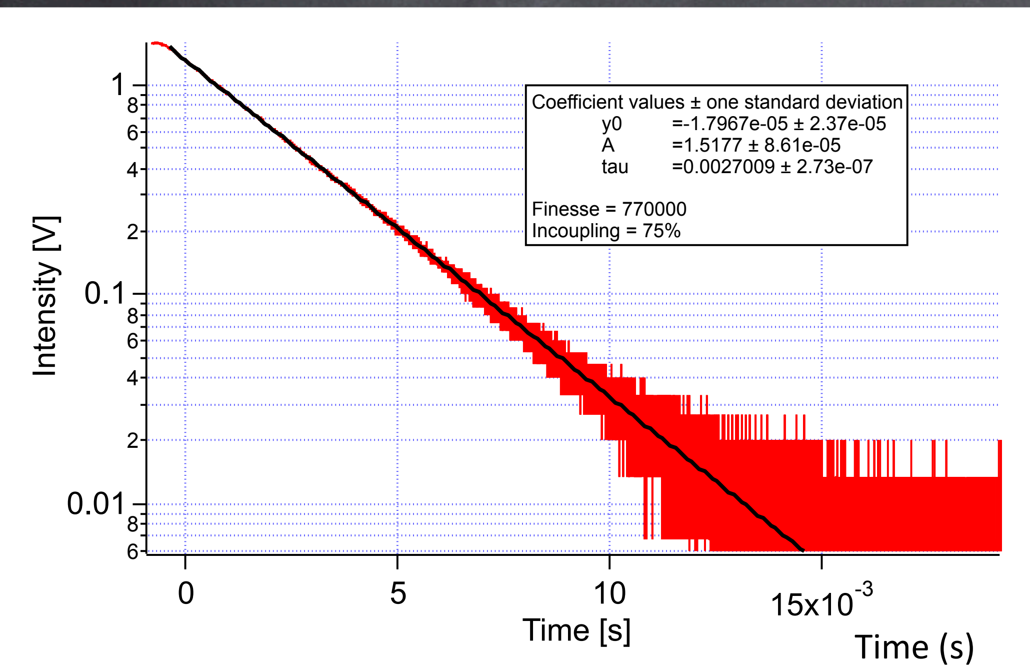

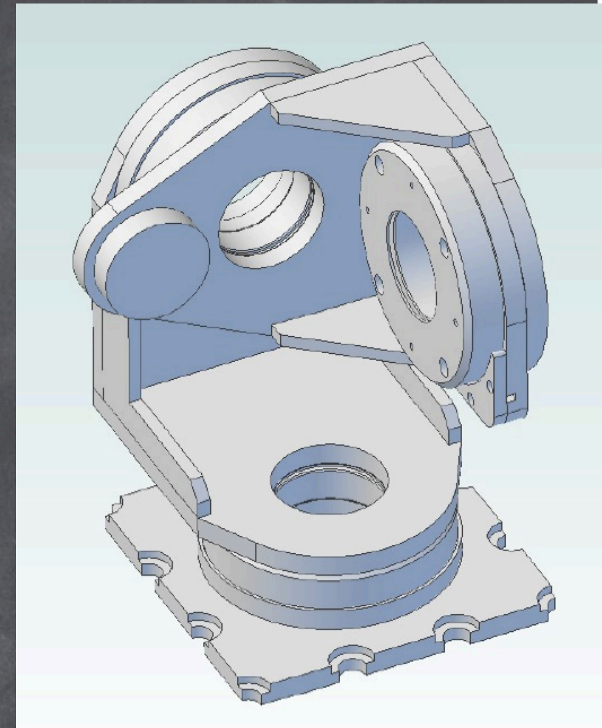

3-Motor Mirror tilter, θ_x, θ_y, θ_z

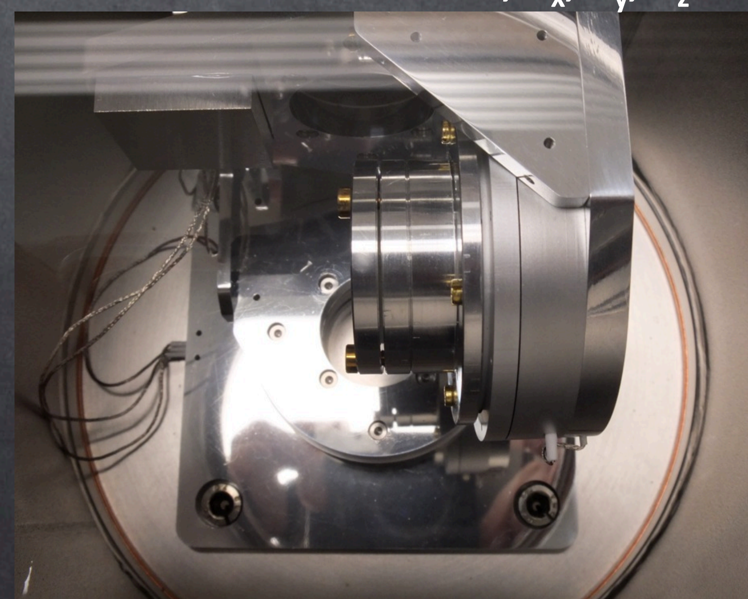

- Transmitted power 25%
- Highest measured finesse = 770 000
  N = 480 000
- τ = 2.7 ms , d = 3.3 m, 65 Hz FWHM

The mounted apparatus

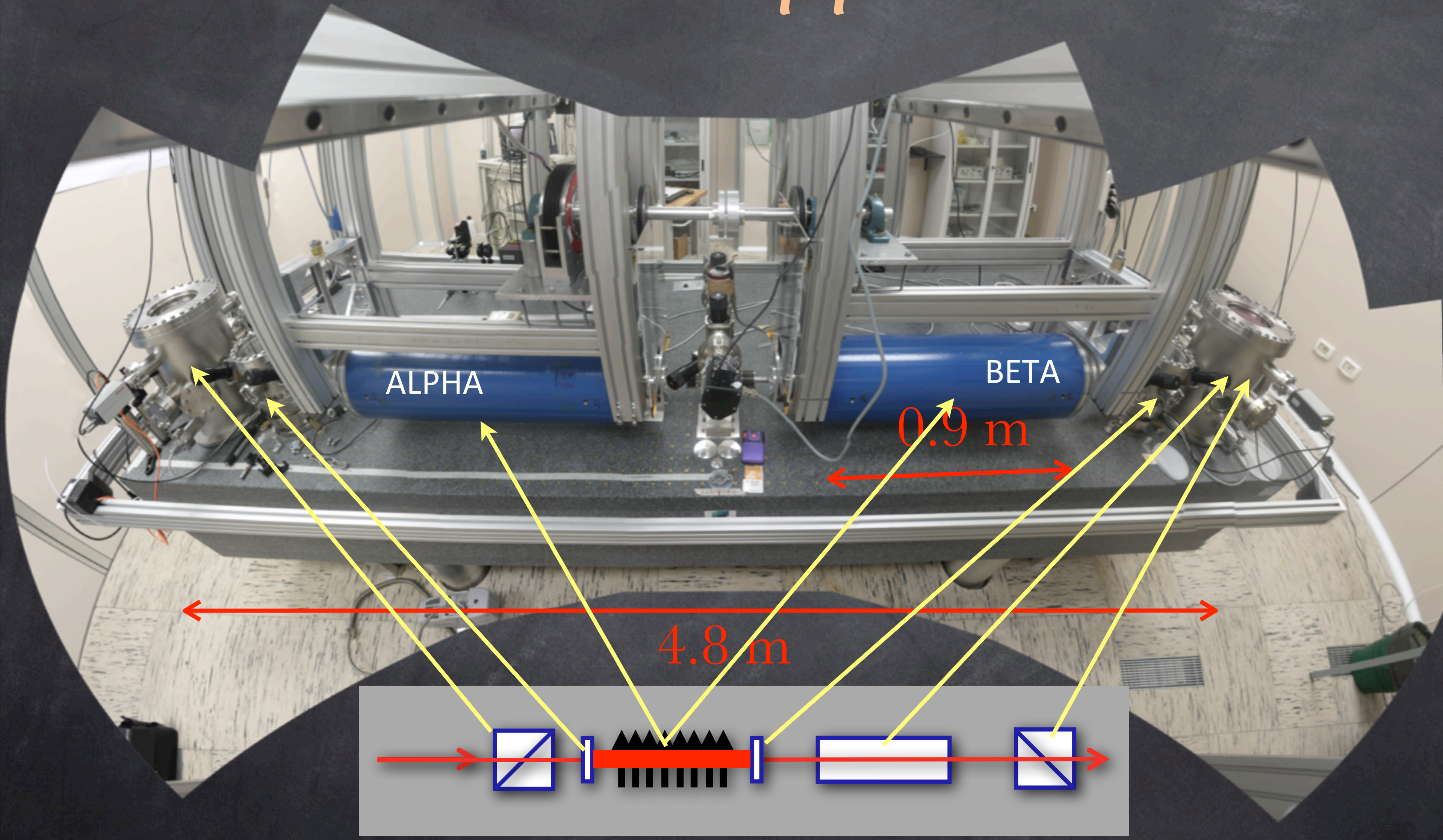

Calibration

Mirror birefringence

Fabry Perot cavity mirrors have **intrinsic static birefringence**

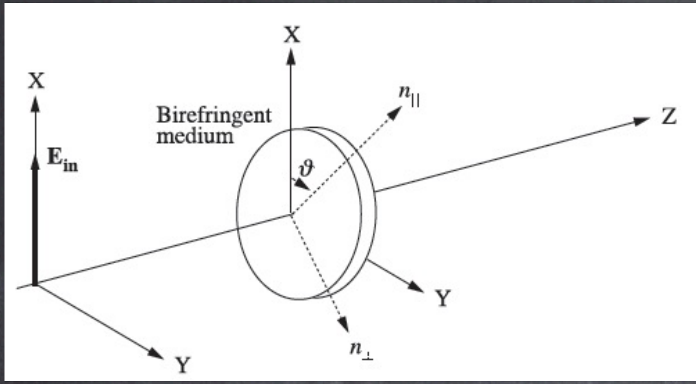

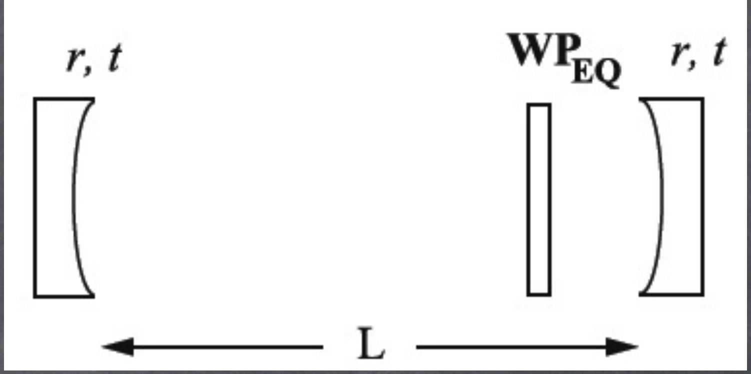

The resulting cavity behaves like a **waveplate.** This results in:

- cavity mode splitting

- increased 1/f noise?

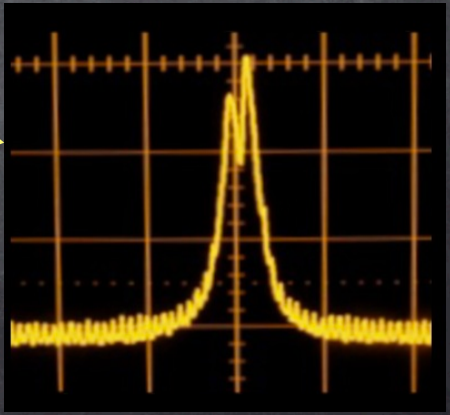

- Cavity mirrors must be rotated to minimise total birefringence
- Polarization must be aligned with one of the equivalent waveplate axes.

Cavity mode splitting mixes ellipticities with rotations

Cavity birefringence

- With He gas at various pressures we measured the ellipticity as a function of the position on the Airy curve (feedback offset).
- No dichroism is induced in He: $\varepsilon = 0$

$$I_{\text{out}} \simeq I_0 \left\{ \sigma^2 + \eta(t)^2 + \eta(t)\alpha(t) + +2\eta(t)\left(\frac{2\mathcal{F}}{\pi}\right)\left[\psi(t) + \left(\frac{2\mathcal{F}}{\pi}\right)\gamma\epsilon(t)\right]\left(\frac{1}{1+\left(\frac{2\mathcal{F}}{\pi}\right)^2 \sin^2\gamma/2}\right)\right\}$$

Error signal

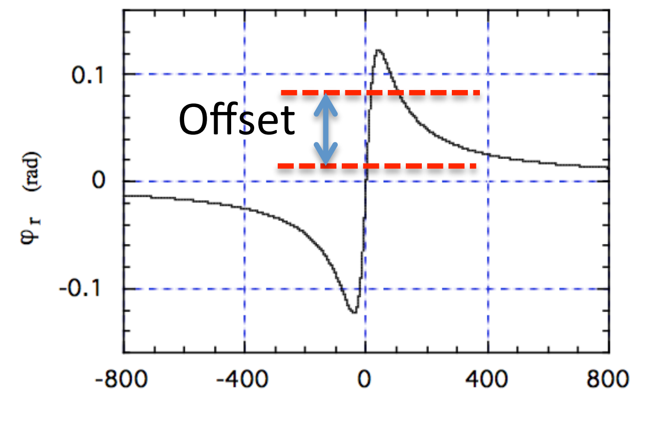

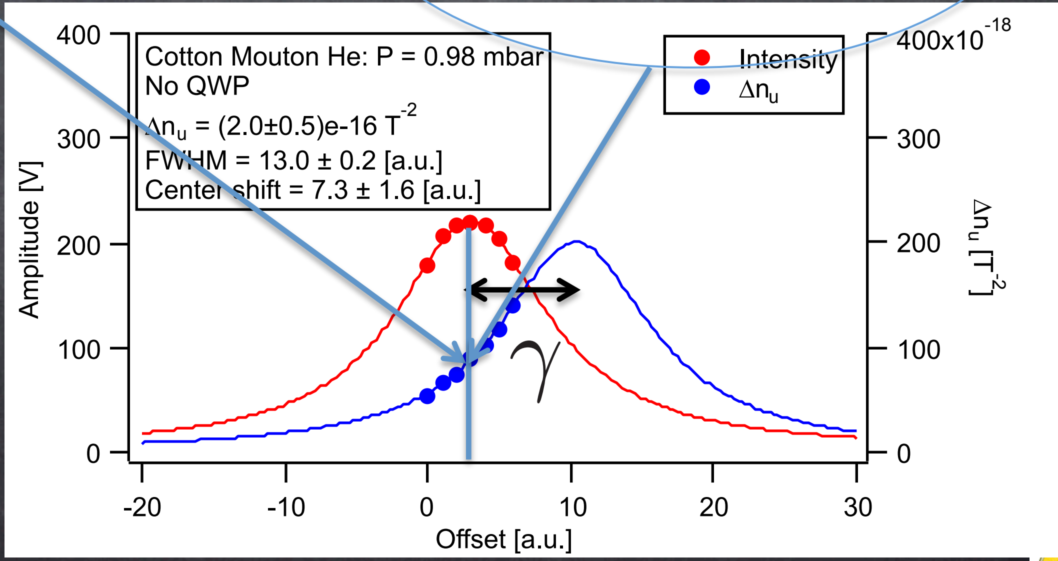

Example with P = 0.98 mbar He

Cavity birefringence

- By inserting a quarter wave plate after the cavity and with He gas at various pressures, we also measured the rotation as a function of feedback offset

$$I_{\rm out} \simeq I_0 \left\{ \sigma^2 + \eta(t)^2 + \eta(t)\alpha(t) + +2\eta(t)\left(\frac{2\mathcal{F}}{\pi}\right)\left[\epsilon(t) - \left(\frac{2\mathcal{F}}{\pi}\right)\gamma\psi(t)\right]\left(\frac{1}{1+\left(\frac{2\mathcal{F}}{\pi}\right)^2 \sin^2\gamma/2}\right)\right\}$$

Error signal

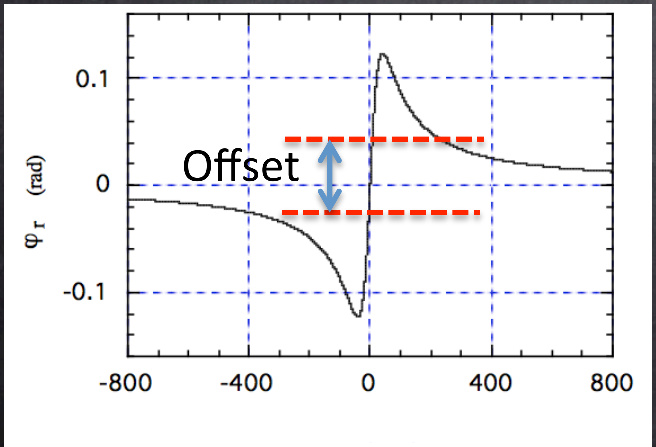

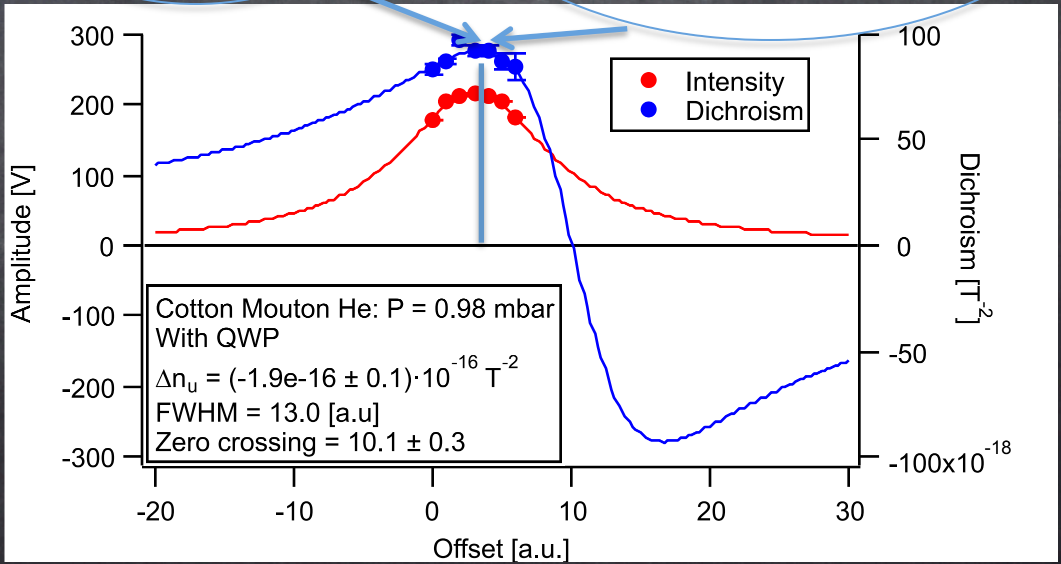

Example with P = 0.98 mbar He

Measurement output

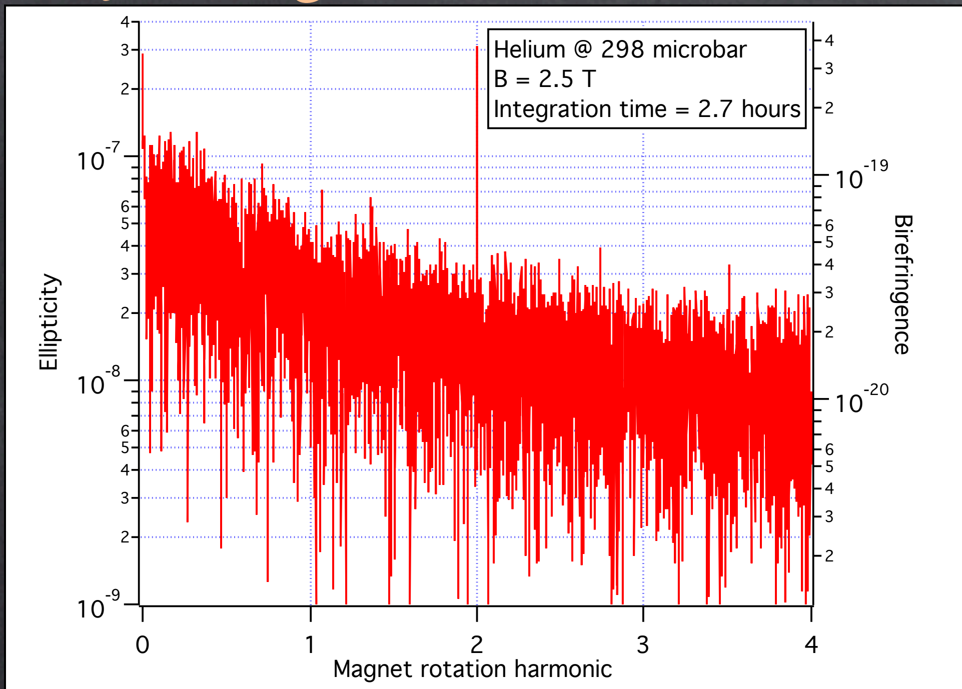

Heterodyne detection technique (Rotating Magnet)

Measured effect given by Fourier amplitude and phase at signal frequency

Vector in the polar plane.

Defines physical axis for any birefringence.

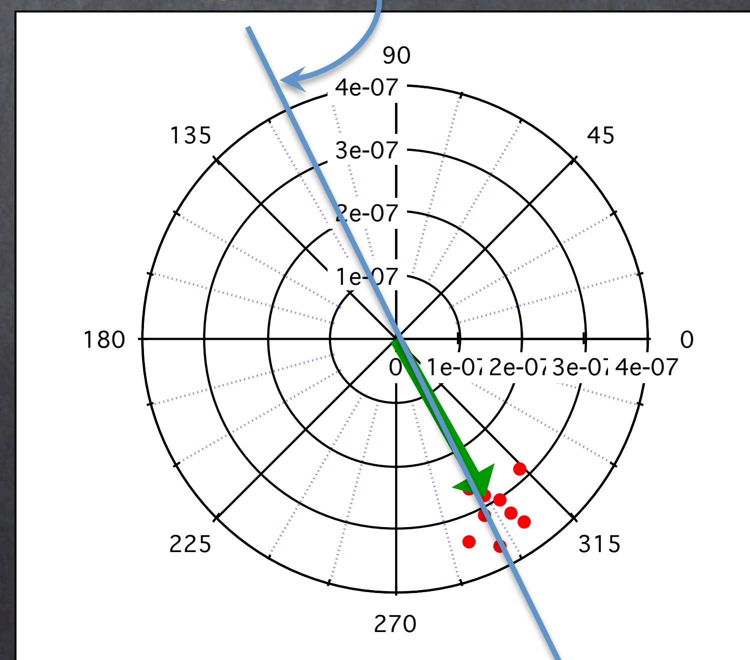

The **amplitude** measures the ellipticity/rotation

The **phase** is related to the acquisition trigger and to the magnetic field direction relative to the polarization. A true physical signal must have a definite phase detremined with gases

$$\psi(t) = \psi_0 \sin(2\omega_{\mathrm{Mag}} + \vartheta_0)$$

Calibration with He

Takes into account the response of the birefringent cavity

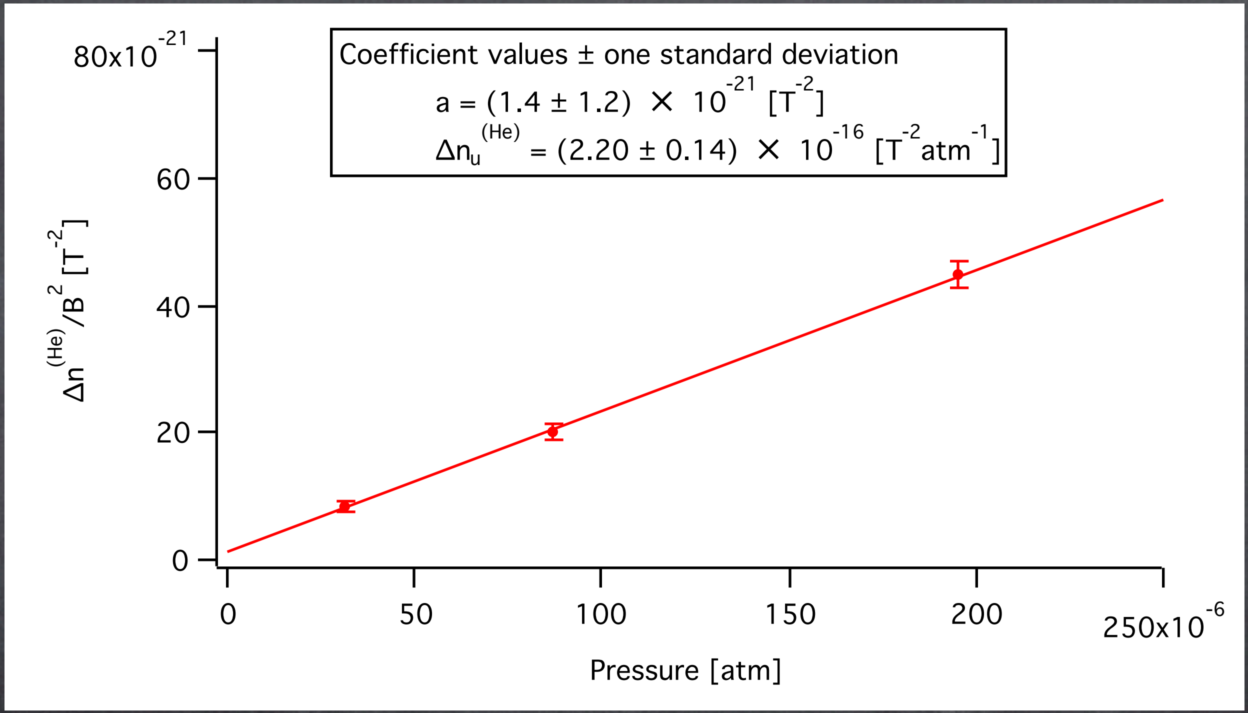

The low pressure point required 5 hours of integration: apparatus is stable.
It corresponds to a birefringence $\Delta n = 8.6 \cdot 10^{-21}$

Vacuum results

Spectrum of obtained data around signal frequency

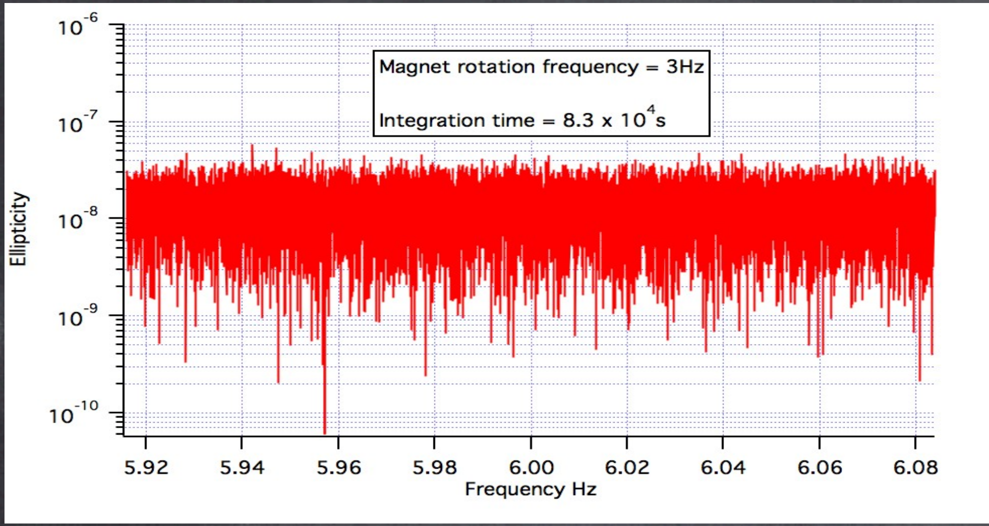

Distribution of noise
Rayleigh function

$$P(r) = N \frac{r}{\sigma_\psi^2} e^{-\frac{r^2}{2\sigma_\psi^2}}$$

$\sigma_\psi = 1.1\ 10^{-8}$

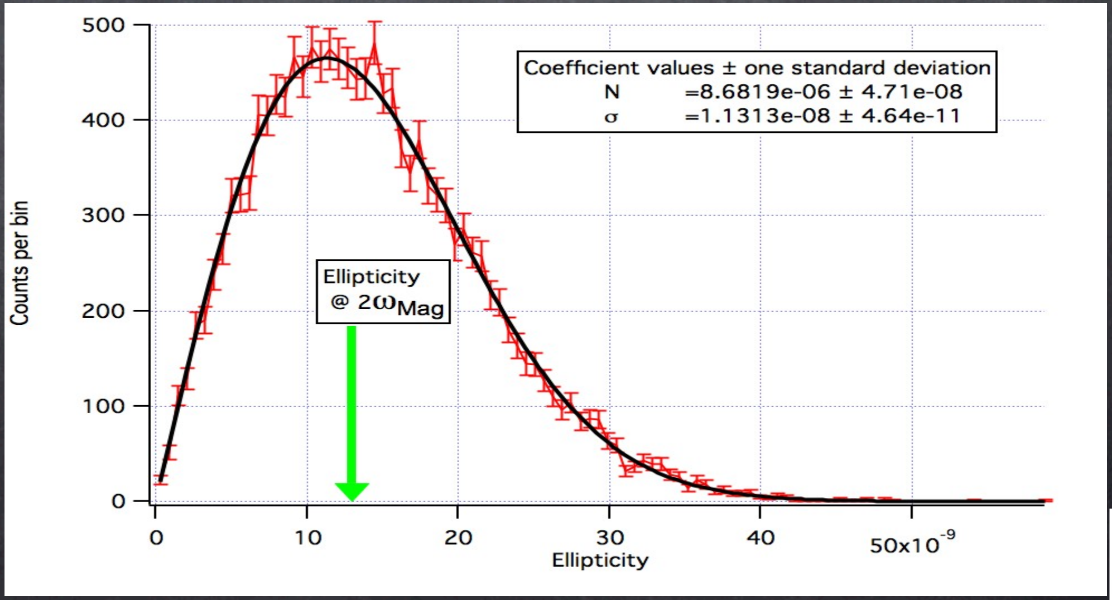

Ellipticity data

Run #	Quantity	Magnets	$2\nu_B$ (Hz)	T (s)	$\mathcal{F}$	$k(\alpha)$
0	ψ	MA + MB		6.7×10^5	6.7×10^5	0.50
1	ψ	MB	8	1.0×10^6	7.0×10^5	0.65
2	ψ	MA	10	1.0×10^6	7.0×10^5	0.65
3	ψ	MB	10	8.9×10^5	7.0×10^5	0.65
4	ψ	MA	12.5	8.9×10^5	7.0×10^5	0.65
5	θ	MA + MB	10	1.4×10^5	7.0×10^5	0.65

2014 ellipticity data. (PRD **90** (2014) 092003)

2015 Ellipticity measurements without QWP

2015 Rotation measurement with QWP

Run #	Quantity	In-phase	Quadrature	σ	$S_{2\nu_B}^{\mathrm{meas}}$ $(1/\sqrt{\mathrm{Hz}})$
0	ψ	$+5.2 \times 10^{-10}$	$+6.5 \times 10^{-10}$	2.6×10^{-9}	2.1×10^{-6}
2	ψ	-6.9×10^{-11}	$+2.6 \times 10^{-10}$	4.9×10^{-10}	4.9×10^{-7}
3	ψ	-4.1×10^{-10}	$+1.0 \times 10^{-9}$	5.4×10^{-10}	5.1×10^{-7}
5	θ (rad)	-6.6×10^{-11}	-1.9×10^{-9}	1.3×10^{-9}	4.8×10^{-7}
$0'$	θ (rad)	$+5.2 \times 10^{-10}$		2.6×10^{-9}	2.1×10^{-6}
$2'$	θ (rad)	-9.4×10^{-11}		6.7×10^{-10}	6.7×10^{-7}
$3'$	θ (rad)	-5.6×10^{-10}		7.4×10^{-10}	6.9×10^{-7}
$5'$	ψ	$+9.0 \times 10^{-11}$		1.8×10^{-9}	6.5×10^{-7}

Birefringence - dichroism data

Run #	Quantity	In-phase	Quadrature	σ	$S_{2\nu_B}^{\text{meas}}$ $(1/\sqrt{\text{Hz}})$
0	Δn	$+2.5 \times 10^{-22}$	$+3.1 \times 10^{-22}$	1.3×10^{-21}	1.0×10^{-18}
2	Δn	-6.4×10^{-23}	$+2.4 \times 10^{-22}$	4.5×10^{-22}	4.5×10^{-19}
3	Δn	-3.8×10^{-22}	$+9.3 \times 10^{-22}$	5.0×10^{-22}	4.7×10^{-19}
$5'$	Δn	$+4.2 \times 10^{-23}$		8.2×10^{-22}	3.0×10^{-19}
$0'$	$\Delta \kappa$	$+2.5 \times 10^{-22}$		1.3×10^{-21}	1.0×10^{-18}
$2'$	$\Delta \kappa$	-8.7×10^{-23}		6.2×10^{-22}	6.2×10^{-19}
$3'$	$\Delta \kappa$	-5.2×10^{-22}		6.8×10^{-22}	6.4×10^{-19}
5	$\Delta \kappa$	-3.1×10^{-23}	-8.8×10^{-22}	6.0×10^{-22}	2.2×10^{-19}

Della Valle et al., EPJ C, (2016) 76:24

- Birefringence and dichroisms for 2.5 T
- Unitary birefringence $\Delta n_u = \dfrac{\Delta n}{B^2}$

Averages

$$\boxed{\begin{aligned}\Delta n^{(\text{PVLAS})} &= (-1.5 \pm 3.0) \times 10^{-22} \\ \Delta \kappa^{(\text{PVLAS})} &= (-1.6 \pm 3.5) \times 10^{-22}\end{aligned}}$$

PVLAS combined best value

PVLAS best value: $\Delta n_u^{(\mathrm{vac})} = (-24 \pm 48) \times 10^{-24}\ \mathrm{T}^{-2}$

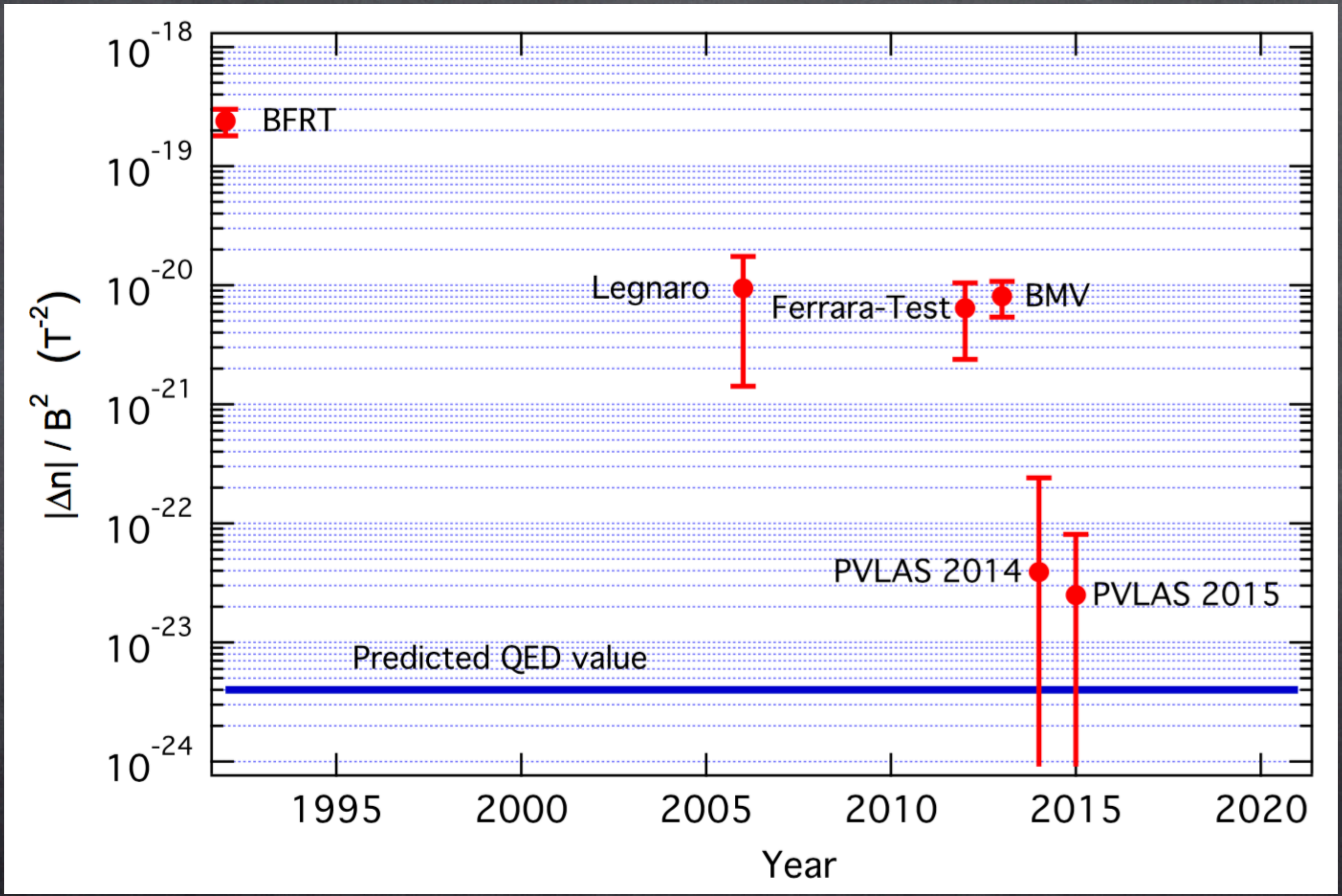

Della Valle et al., EPJ C, (2016) 76:24

$$\Delta n_u^{(\mathrm{qed})} = 3A_e = +3.96 \times 10^{-24}\ \mathrm{T}^{-2}$$

Axion-like particles

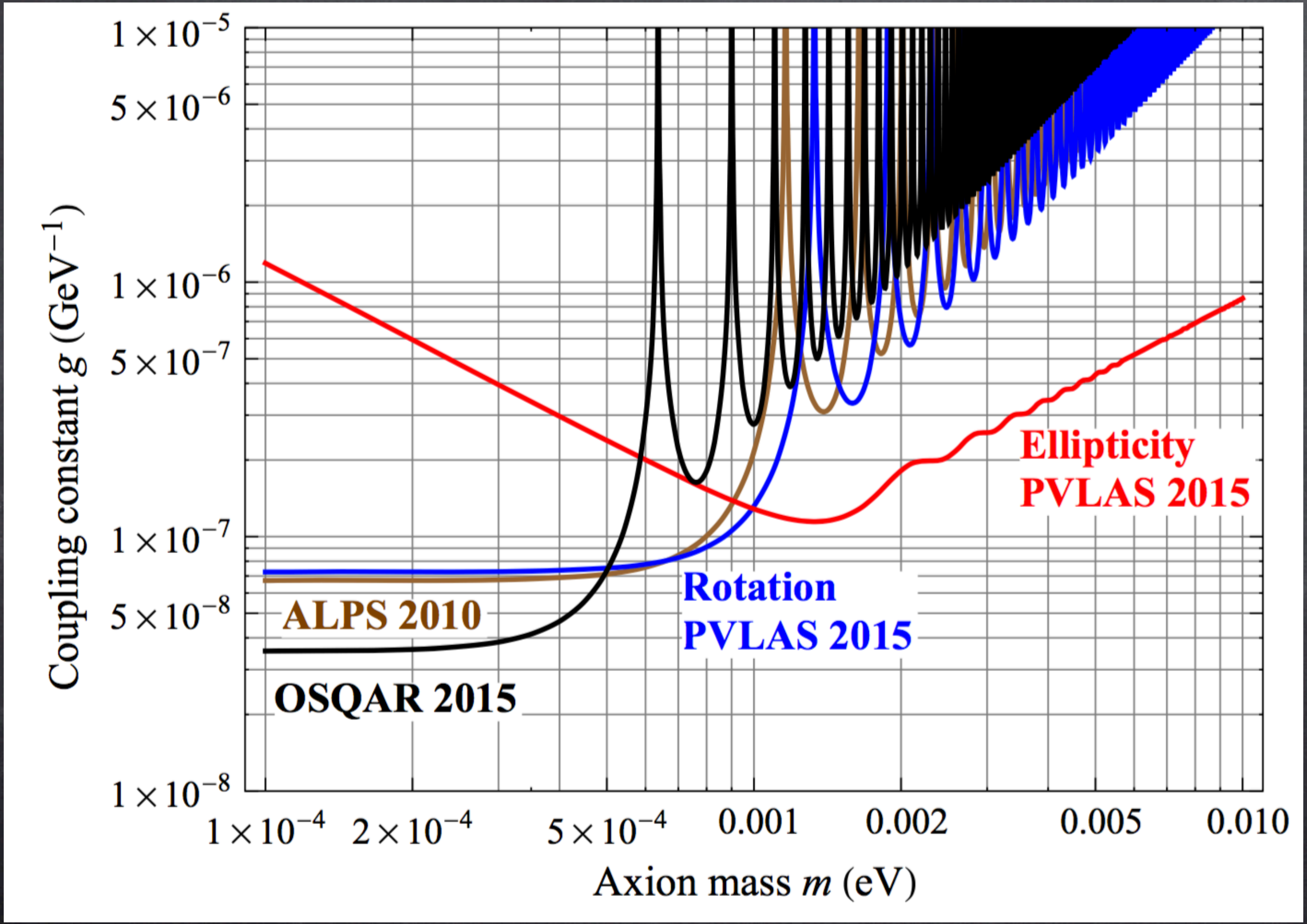

Della Valle et al., EPJ C, (2016) 76:24

Thank you for your attention